Regular Article

Qasim Abbas Atiyah* and Imad Abdulhussein Abdulsahib

Compressive forces influence on the vibrations of double beams

https://doi.org/10.1515/eng-2022-0408
received July 22, 2022; accepted January 25, 2023

Abstract: The influence of compressive forces on the lower and upper natural frequencies of the double beams has been studied in this article. Euler–Bernoulli's hypotheses have been used to derive the natural frequency equations. Two asymmetric beams were assumed in this work, and four different boundary conditions were applied in these equations: Pinned–Pinned, Clamped–Clamped, Clamped–Free, and Clamped–Pinned. When the axial compressive force is increased about 18 times, it is observed that the lower natural frequencies decreased by 19% for PP beam, 8% for CC beam, 81% for CF beam, and 12% for CP beam. However, the greatest effect of the axial force on the higher frequencies is by reducing it in the CC beam by a ratio that does not exceed 2%. A rise in the values of axial compressive force causes a reduction in the lower natural frequencies, mostly for the CF beam, while it has a little effect on the higher natural frequencies. Similarly, when the compressive forces on the upper and lower beams fluctuate simultaneously, their effect is doubled on the frequencies when the axial compressive force on one of the two beams changes only.

Keywords: double beam, vibration of beam, compressive force

1 Introduction

The double beam is considered one of the relatively recent developments in the field of creating materials that have unique properties of high resistance to stress and shock through the two outer layers and high flexibility with the light weight of the inner layer connecting between these two layers, which gave it a high resistance to bear the stresses of buckling and bending and gave these materials a wide space for engineering applications in aerospace fields such as aircraft structures, marine applications, the automotive industry, and structural applications. The vibration of beam constructions is essential in mechanical, civil, and aeronautical engineering. A double beam is a type of composite beam construction that is linked together to form a single beam. For different purposes, the beam's thickness and material qualities may vary. Zhang et al. [1,2] evaluated the vibrations of a coupled S.S double-beam system under compressive load using Bernoulli–Euler beam theory. A Winkler elastic layer is supposed to connect the two beams of the system indefinitely. The system's dynamic reactions to arbitrarily disperse continuous loads were determined, for two situations with specific excitation loadings. Zhao et al. [3–5] investigated the closed-form solutions of a Timoshenko double-beam forced transverse vibration under compressive axial stress. The two beams are represented by the Timoshenko model. The steady-state of the linked double-beam system was derived from the Laplace transform. Mao and Wattanasakulpong [6,7] evaluated the free vibration of a cantilever double-beam system that is constantly linked. The differential equations for the double beam were expressed as a recursive algebraic equation based on the AMDM. Fei et al. [8–10] investigated the vibration properties of inclined double-beam. Two elastic beams make up the double-beam system of varying mass which are connected by elastic springs. A tensile axial force was used on the beam with the higher rigidity mass. The dynamic equations of the double beam were developed by concurrently taking into account the effects of stiffness, sag, and other parameters. The element and stiffness matrix was generated from the governing equations to get the dynamic balance equations of the system. Sari et al. [11] studied the free vibration and stability assessments of single and double composite beams. A constant axially compressive or tensile force was applied to the closed-section beams. A layer of rotational and translational springs is supposed to link the twin beams. The discretization process was utilized to find the

*** Corresponding author: Qasim Abbas Atiyah,** Mechanical Engineering Department, University of Technology, Baghdad, Iraq, e-mail: qasim.a.atiyah@uotechnology.edu.iq
Imad Abdulhussein Abdulsahib: Mechanical Engineering Department, University of Technology, Baghdad, Iraq, e-mail: imad.a.abdulsahib@uotechnology.edu.iq

partial differential equations. On the mode forms, the critical loads, natural frequencies, impacts of elastic layer characteristics, axial forces, and boundary conditions have been examined. Stojanović et al. [12,13] investigated the effects of rotating inertia on the vibration and buckling of a double beam. The starting value and boundary value difficulties have been solved. An elastically coupled double-beam complex system's natural frequencies and amplitude ratios were determined. The influence of physical characteristics describing the vibrating system on the natural frequency, critical buckling load, and amplitude ratios was examined in the theoretical analysis. Kozić et al. [14] prepossessed an analytical method for defining the properties of coupled parallel beams subjected to axial force. For a complicated system, the amplitude ratio, natural frequencies, and critical buckling stress were calculated. Abdulsahib and Abbas Atiyah [15,16] investigated the influence of non-linear elasticity on the frequency of sandwich beams with arbitrary boundary conditions. The energy balancing technique was used to calculate the effect of the inner layer's non-linearity stiffness on those frequencies. The behavior of the higher and lower natural frequencies of the asymmetric doubled beams will be studied under various boundary conditions, with the influence of a number of properties, such as the difference in thickness of the two beams, their mass densities, their elasticity modulus, the properties of the connected layer between them, or the length of beams. Milenković et al. [17] studied the natural frequencies of a Rayleigh double-beam system with a Keer layer in-between and the influence of axial stress. It was considered that the system's two beams being continually linked by a Keer layer. The system's equations of motion were defined by a number of differential equations. The standard Bernoulli–Fourier approach was employed to resolve these equations, and the Rayleigh theory was applied to derive the natural frequency and amplitude ratio of the examined model. Abbas Atiyah and Abdulsahib [18,19] examined the effect of four geometric and material properties on the twin beam vibration. The intermediate layer's properties, as well as the mass density, thickness, and modulus of elasticity of the two beams, were investigated. The Bernoulli–Euler beam equation was used to calculate the frequencies of the twin beams. In this article, the influence of the axial compressive forces on the lower and higher natural frequencies of the double beams was studied. Euler–Bernoulli's hypotheses have been used to derive the natural frequency equations. Two asymmetric beams were assumed in this work, and four different boundary conditions were applied in these equations: Pinned–Pinned, Clamped–Clamped, Clamped–Free, and Clamped–Pinned.

2 Theoretical work

Assuming two asymmetric beams joined by an elastic layer. Compressive axial loads are applied to both ends of each beam (F_1) and (F_2), respectively. Each beam has a different thickness (h), mass density (ρ), and modulus of elasticity (E), as shown in Figure 1. The two beams have the same length (L) and width (b). The Bernoulli–Euler beam theory was used to find the equations of motion as follows:

$$\frac{\partial^2}{\partial x^2}\left(E_1 I_1 \frac{\partial^2 W_1}{\partial x^2}\right) + K(W_1 - W_2) + \rho_1 A_1 \frac{\partial^2 W_1}{\partial t^2} + F_1 \frac{\partial^2 W_1}{\partial x^2} = 0, \tag{1}$$

$$\frac{\partial^2}{\partial x^2}\left(E_2 I_2 \frac{\partial^2 W_2}{\partial x^2}\right) - K(W_1 - W_2) + \rho_2 A_2 \frac{\partial^2 W_2}{\partial t^2} + F_2 \frac{\partial^2 W_2}{\partial x^2} = 0, \tag{2}$$

where, $A_1, A_2, E, I_1, I_2, W_1$, and W_2 are the cross-sectional areas, modulus of elasticity, moments of area, and the deflection for the upper and lower beam, respectively.

The following Boundary conditions were used in this work:

For Cantilever (Pinned–Free) beam:

$$W_1(0,t) = \acute{W}_1(0,t) = \acute{\acute{W}}_1(L,t) = \acute{\acute{\acute{W}}}_1(L,t) = 0, \tag{3}$$

$$W_2(0,t) = \acute{W}_2(0,t) = \acute{\acute{W}}_2(L,t) = \acute{\acute{\acute{W}}}_2(L,t) = 0, \tag{4}$$

For Pinned–Pinned beam:

$$W_1(0,t) = \acute{W}_1(0,t) = W_1(L,t) = \acute{W}_1(L,t) = 0 \tag{5}$$

$$W_2(0,t) = \acute{W}_2(0,t) = W_2(L,t) = \acute{W}_2(L,t) = 0 \tag{6}$$

For Simply supported-Simply supported beam:

$$W_1(0,t) = \acute{\acute{W}}_1(0,t) = W_1(L,t) = \acute{\acute{W}}_1(L,t) = 0, \tag{7}$$

$$W_2(0,t) = \acute{\acute{W}}_2(0,t) = W_2(L,t) = \acute{\acute{W}}_2(L,t) = 0. \tag{8}$$

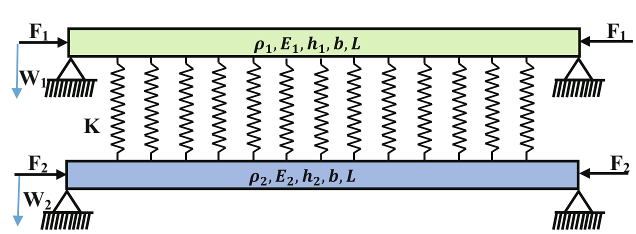

Figure 1: Asymmetric double beam with compressive loads on ends.

For Free–Free beam:

$$W_1''(0,t) = W_1'''(0,t) = W_1''(L,t) = W_1'''(L,t) = 0, \tag{9}$$

$$W_1''(0,t) = W_1'''(0,t) = W_1''(L,t) = W_1'''(L,t) = 0. \tag{10}$$

For Pinned-simply Supported beam:

$$W_1(0,t) = W_1'(0,t) = W_1(L,t) = W_1''(L,t) = 0, \tag{11}$$

$$W_2(0,t) = W_2'(0,t) = W_2(L,t) = W_2''(L,t) = 0. \tag{12}$$

In order to solve equations (1) and (2), the following functions are assumed:

$$W_1(x,t) = \sum_{n=1}^{\infty} X_{n1}(x)\cdot T_{n1}(t), \tag{13}$$

$$W_2(x,t) = \sum_{n=1}^{\infty} X_{n2}(x)\cdot T_{n2}(t). \tag{14}$$

here:

$$T_{n1} = D_1 e^{j\omega_n t}, \tag{15}$$

$$T_{n2} = D_2 e^{j\omega_n t}, \tag{16}$$

$$X_{n1}(x) = C_1 \sin\beta_{n1}x + C_2\cos\beta_{n1}x + C_3\sinh\beta_{n1}x + C_4\cosh\beta_{n1}x, \tag{17a}$$

$$X_{n2}(x) = C_5 \sin\beta_{n2}x + C_6\cos\beta_{n2}x + C_7\sinh\beta_{n2}x + C_8\cosh\beta_{n2}x, \tag{17b}$$

$$\beta_{ni} = \sqrt{\frac{\omega_{ni}^2 \rho_i A_i}{E_i I_i}}, \quad i = 1, 2. \tag{18}$$

When substituting equations (15)–(17) into equations (1) and (2), one gets:

$$\sum_{n=1}^{\infty} \{[(E_1 I_1 \beta_{n1}^4 + K - F_1\beta_{n1}^2) - \rho_1 A_1 \omega_n^2] T_{n1} - K T_{n2}\} X_n, \tag{19}$$

$$\sum_{n=1}^{\infty} \{-K T_{n1} + [(E_2 I_2 \beta_{n2}^4 + K - F_2\beta_{n2}^2) - \rho_2 A_2 \omega_n^2] T_{n2}\} X_n. \tag{20}$$

The differential equations (19) and (20) can be expressed as follows:

$$\left[\left(\frac{E_1 I_1 \beta_{n1}^4 + K}{\rho_1 A_1} - \frac{\beta_{n1}^2}{\rho_1 A_1}F_1\right) - \omega_n^2\right] D_1 - \frac{K}{\rho_1 A_1} D_2 = 0, \tag{21}$$

$$-\frac{K}{\rho_2 A_2} D_1 + \left[\left(\frac{E_2 I_2 \beta_{n2}^4 + K}{\rho_2 A_2} - \frac{\beta_{n2}^2}{\rho_2 A_2}F_2\right) - \omega_n^2\right] D_2 = 0. \tag{22}$$

Equations (20) and (21) can be expressed in matrix form as follows:

$$\begin{bmatrix} \left(\frac{E_1 I_1 \beta_{n1}^4 + K}{\rho_1 A_1} - \frac{\beta_{n1}^2}{\rho_1 A_1}F_1\right) - \omega_n^2 & -\frac{K}{\rho_1 A_1} \\ -\frac{K}{\rho_2 A_2} & \left(\frac{E_2 I_2 \beta_{n2}^4 + K}{\rho_2 A_2} - \frac{\beta_{n2}^2}{\rho_2 A_2}F_2\right) - \omega_n^2 \end{bmatrix} \begin{bmatrix} D_1 \\ D_2 \end{bmatrix} = \begin{bmatrix} 0 \\ 0 \end{bmatrix}. \tag{23}$$

The non-trivial solution of equation (23) is as follows:

$$\omega_n^4 - \left[\left(\frac{E_1 I_1 \beta_{n1}^4 + K}{\rho_1 A_1} - \frac{\beta_{n1}^2}{\rho_1 A_1}F_1\right) + \left(\frac{E_2 I_2 \beta_{n2}^4 + K}{\rho_2 A_2} - \frac{\beta_{n2}^2}{\rho_2 A_2}F_2\right)\right]^2 + \omega_n^2 + \left[\left(\frac{E_1 I_1 \beta_{n1}^4 + K}{\rho_1 A_1} - \frac{\beta_{n1}^2}{\rho_1 A_1}F_1\right)\left(\frac{E_2 I_2 \beta_{n2}^4 + K}{\rho_2 A_2} - \frac{\beta_{n2}^2}{\rho_2 A_2}F_2\right) - \frac{K^2}{\rho_1 A_1 \rho_2 A_2}\right] = 0. \tag{24}$$

From equation (24), the lower natural frequency is:

$$\omega_{n1} = \frac{1}{2}\left[\left(\frac{E_1 I_1 \beta_{n1}^4 + K}{\rho_1 A_1} - \frac{\beta_{n1}^2}{\rho_1 A_1}F_1\right) + \left(\frac{E_2 I_2 \beta_{n2}^4 + K}{\rho_2 A_2} - \frac{\beta_{n2}^2}{\rho_2 A_2}F_2\right)\right] - \sqrt{\begin{matrix}\left[\left(\frac{E_1 I_1 \beta_{n1}^4 + K}{\rho_1 A_1} - \frac{\beta_{n1}^2}{\rho_1 A_1}F_1\right) + \left(\frac{E_2 I_2 \beta_{n2}^4 + K}{\rho_2 A_2} - \frac{\beta_{n2}^2}{\rho_2 A_2}F_2\right)\right]^2 \\ - 4\left[\left(\frac{E_1 I_1 \beta_{n1}^4 + K}{\rho_1 A_1} - \frac{\beta_{n1}^2}{\rho_1 A_1}F_1\right)\left(\frac{E_2 I_2 \beta_{n2}^4 + K}{\rho_2 A_2} - \frac{\beta_{n2}^2}{\rho_2 A_2}F_2\right) - \frac{K^2}{\rho_1 A_1 \rho_2 A_2}\right]\end{matrix}}. \tag{25}$$

And, the higher natural frequency is:

$$\omega_{n2} = \frac{1}{2}\left[\left(\frac{E_1I_1\beta_{n1}^4 + K}{\rho_1A_1} - \frac{\beta_{n1}^2}{\rho_1A_1}F_1\right) + \left(\frac{E_2I_2\beta_{n2}^4 + K}{\rho_2A_2} - \frac{\beta_{n2}^2}{\rho_2A_2}F_2\right)\right] + \sqrt{\begin{array}{l}\left[\left(\frac{E_1I_1\beta_{n1}^4 + K}{\rho_1A_1} - \frac{\beta_{n1}^2}{\rho_1A_1}F_1\right) + \left(\frac{E_2I_2\beta_{n2}^4 + K}{\rho_2A_2} - \frac{\beta_{n2}^2}{\rho_2A_2}F_2\right)\right]^2 \\ - 4\left[\left(\frac{E_1I_1\beta_{n1}^4 + K}{\rho_1A_1} - \frac{\beta_{n1}^2}{\rho_1A_1}F_1\right)\left(\frac{E_2I_2\beta_{n2}^4 + K}{\rho_2A_2} - \frac{\beta_{n2}^2}{\rho_2A_2}F_2\right) - \frac{K^2}{\rho_1A_1\rho_2A_2}\right]\end{array}}. \quad (26)$$

When applying the boundary conditions in equations (7)–(14), the following shape functions can be obtained [33]:

$$\begin{aligned} X_n(x) &= \cos h(\beta_n x) - \cos(\beta_n x) \\ &\quad - \sigma_n[\sin h(\beta_n x) - \sin(\beta_n x)], \\ \beta_n &= \frac{\pi(2n+1)}{2}, n = 1, 2, 3, \ldots, \\ \sigma_n &\cong 1 \text{ for Clamped beams,} \end{aligned} \quad (27)$$

$$X_n(x) = \sin(\beta_n x), \quad \beta_n = n\pi, \quad n = 1, 2, 3, \ldots \text{ for Pinned beams,} \quad (28)$$

$$\begin{aligned} X_n(x) &= \cos h(\beta_n x) + \cos(\beta_n x) \\ &\quad - \sigma_n[\sin h(\beta_n x) + \sin(\beta_n x)], \\ \beta_n &= \frac{\pi(2n+1)}{2}, n = 1, 2, 3, \ldots, \\ \sigma_n &\cong 1 \text{ for Free beams,} \end{aligned} \quad (29)$$

$$\begin{aligned} X_n(x) &= \cos h(\beta_n x) - \cos(\beta_n x) \\ &\quad - \sigma_n[\sin h(\beta_n x) - \sin(\beta_n x)], \\ \beta_n &= \frac{\pi(2n-1)}{2}, n = 1,2,3, \ldots, \\ \sigma_n &\cong 1 \text{ for Cantilever beam,} \end{aligned} \quad (30)$$

$$\begin{aligned} X_n(x) &= \cos h(\beta_n x) - \cos(\beta_n x) \\ &\quad - \sigma_n[\sin h(\beta_n x) - \sin(\beta_n x)], \\ \beta_n &= \frac{\pi(4n+1)}{4}, n = 1,2,3, \ldots, \\ \sigma_n &\cong 1 \text{ for Clamped} - \text{Pinned beams.} \end{aligned} \quad (31)$$

3 Results and discussions

Table 1 shows the first lower and higher eight natural frequency values for a double beam under compressive axial load for PP, CC, CF, and CP boundary conditions.

The influence of the axial compressive force on the natural frequencies can be seen in Figures 2 and 3, and Table 2. When the axial compressive force is increased from 2,000 to 38,000 N, it is noticed that the lower natural frequencies decreased by 19% for the PP beam, 8% for the CC beam, 81% for the CF beam, and by 12% for the CP beam. While the greatest effect of the compressive force on the higher frequencies is by reducing it in the CC beam by a ratio that does not exceed 2%. Therefore, it can be concluded that the axial compressive force has a clear effect by reducing the lower natural frequencies,

Table 1: First six lower and higher natural frequencies for double beam

No.of mode	PP Beam		CC Beam		CF Beam		CP Beam	
	L	*H*	*L*	*H*	*L*	*H*	*L*	*H*
1	27.734	103.774	63.184	118.288	9.720	100.471	43.465	109.038
2	111.678	149.906	174.600	201.210	62.223	117.778	141.407	173.194
3	251.583	270.728	342.523	356.822	174.669	201.269	295.302	311.774
4	447.449	458.487	566.368	575.128	342.518	356.817	505.157	514.960
5	699.277	706.391	846.177	852.065	566.366	575.126	770.972	777.430

$\rho_1 = \rho_2 = 2{,}000$ kg/m^3, $E_1 = E_2 = 1 \times 10^{11}$ N/m^2, $K = 10^5$ N/m^2, $F_1 = F_2 = 1{,}000$ N, $L = 6$ m, $b = 0.2$ m, $h = 0.05$ m.

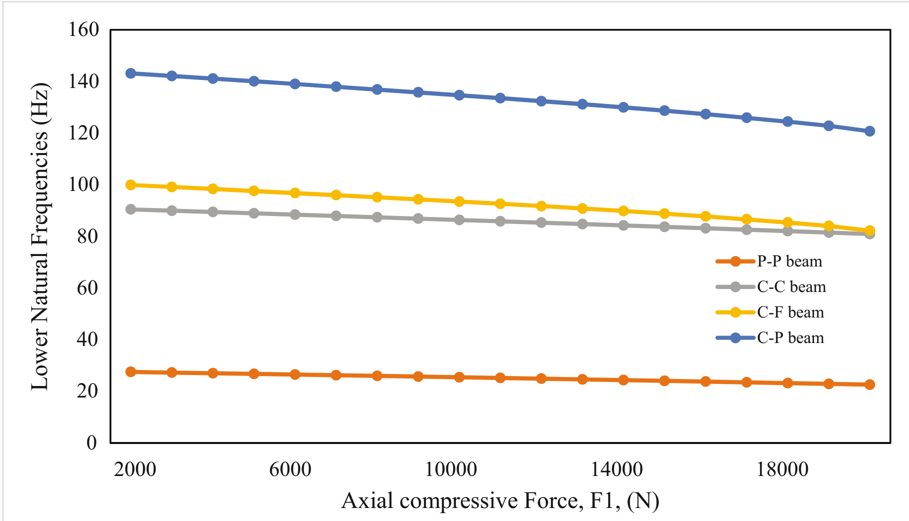

Figure 2: Lower natural frequency vs the axial compressive force (F_1).

especially for the CF beam, and its effect is almost marginal on the higher frequencies. The same effect and behavior of the frequencies were observed when the axial compressive force on the upper beam of the double beam changed with the stability of the force value on the lower beam or when the effect was reversed by changing the compressive force on the lower beam and fixing it on the upper beam.

Figures 4 and 5, and Table 3 depict the behavior of the changing in natural frequencies when changing the values of the axial compressive forces on the upper and lower beams with the same values.

When the values of the axial forces are increased from 2,000 to 20,000, a decrease in the values of low natural frequencies is observed by 18% for the PP beam, 8% for the CC beam, 86% for the CF beam, and 11% for the CP beam. The greatest effect of changing the values of the axial compressive force on the higher natural frequencies when its values change symmetrically from 2,000 to 20,000 N for the CC beam causes it to decrease by less than 2%. A rise in the axial compressive force causes a lessening in the lower natural frequencies, particularly for the CF beam, while it has so little influence on the higher natural frequencies. Likewise, when the compressive forces on the upper and lower beams fluctuate at the same time, their effect is doubled on the frequencies when the axial compressive force on one of the two beams changes only.

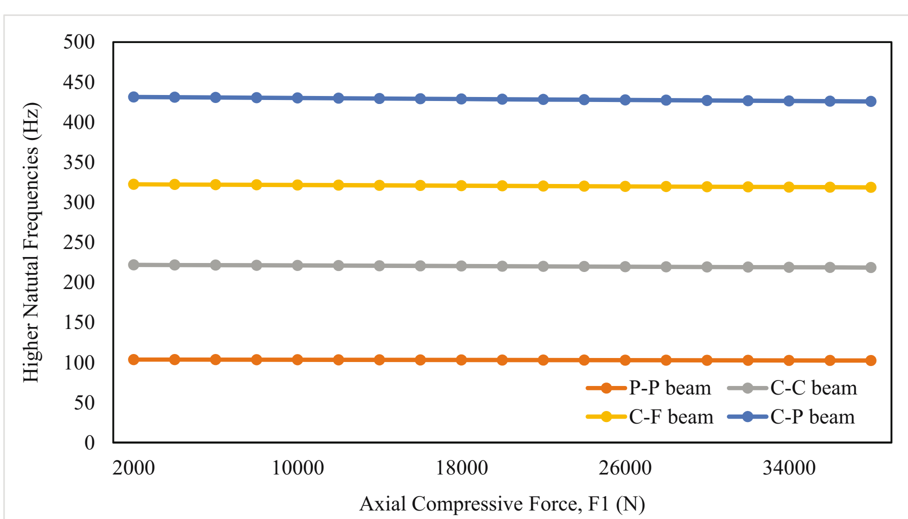

Figure 3: Higher natural frequency vs the axial compressive force (F_1).

Table 2: The natural frequencies vs the axial compressive force

F_1 (N)	PP Beam		CC Beam		CF Beam		CP beam	
	L	*H*	*L*	*H*	*L*	*H*	*L*	*H*
2,000	27.61095	103.7419	63.0608	118.2232	9.59361	100.4591	43.34236	108.9889
4,000	27.36091	103.6760	62.8124	118.0925	9.33538	100.4349	43.09355	108.8910
6,000	27.10786	103.6102	62.5615	117.9625	9.06953	100.4106	42.84223	108.7935
8,000	26.85174	103.5446	62.3080	117.8332	8.79538	100.3863	42.58835	108.6963
10,000	26.59244	103.4791	62.05197	117.7045	8.51213	100.3621	42.33186	108.5995
12,000	26.32987	103.4137	61.79327	117.5766	8.21883	100.3379	42.07272	108.5029
14,000	26.06393	103.3485	61.53191	117.4493	7.91436	100.3137	41.81088	108.4068
16,000	25.79453	103.2835	61.26787	117.3227	7.59739	100.2895	41.54628	108.3109
18,000	25.52155	103.2185	61.0011	117.1967	7.26628	100.2654	41.27888	108.2154
20,000	25.24487	103.1537	60.73158	117.0715	6.91900	100.2412	41.00862	108.1202
22,000	24.96438	103.0891	60.45927	116.947	6.55298	100.2171	40.73545	108.0254
24,000	24.67993	103.0246	60.18414	116.8231	6.16488	100.1930	40.4593	107.9309
26,000	24.39141	102.9602	59.90614	116.6999	5.75023	100.1689	40.18011	107.8367
28,000	24.09864	102.896	59.62524	116.5775	5.30281	100.1448	39.89783	107.7429
30,000	23.80149	102.8319	59.3414	116.4557	4.81349	100.1208	39.61239	107.6495
32,000	23.49979	102.7680	59.05458	116.3346	4.26788	100.0968	39.32371	107.5563
34,000	23.19335	102.7042	58.76474	116.2142	3.64077	100.0727	39.03173	107.4635
36,000	22.88199	102.6406	58.47183	116.0945	2.87937	100.0487	38.73638	107.3711
38,000	22.56551	102.5771	58.17583	115.9754	1.82252	100.0248	38.43757	107.2790

$\rho_1 = \rho_2 = 2{,}000\ \text{kg/m}^3$, $E_1 = E_2 = 1 \times 10^{11}\ \text{N/m}^2$, $K = 10^5\ \text{N/m}^2$, $F_2 = 1{,}000$ N, $L = 6$ m, $b = 0.2$ m, $h = 0.05$ m.

The behavior of natural frequencies when the axial compressive force on the upper beam changes and no force acts on the lower beam are shown in Figures 6 and 7 and Table 4. When the axial force is increased from 2,000 to 38,000, the lower natural frequencies decreased by 18% for the PP beam, 9% for the CC beam, 86% for the CF beam, and by 11% for the CP beam. Also, the effect of changing the value of the axial force in this case is so little on the higher natural frequencies and is almost imperceptible. In general, the natural frequencies change in the same proportion when the axial compressive force on one of the two beams changes, whether it is the upper or lower, and the value of the axial force remains constant on the other beam. This change is doubled when the two axial forces applied to the two beams change with the same value.

From the foregoing, it can be concluded that the effect of the axial force on the natural frequencies is clear when one end of the beam is free, and this effect is negligible if the two ends are fixed, especially if both are

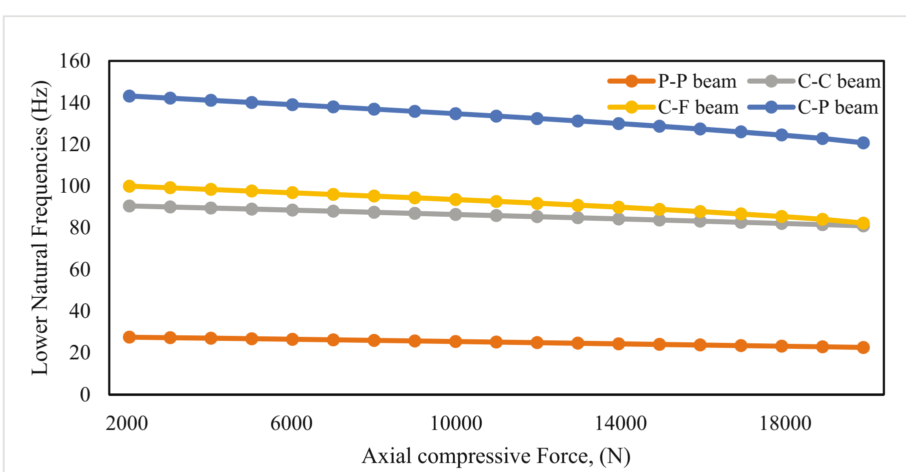

Figure 4: Lower natural frequency vs the axial compressive forces (F_1 and F_2).

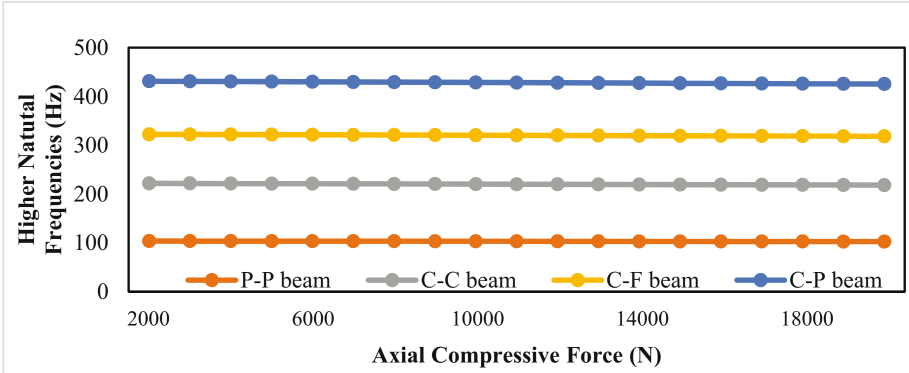

Figure 5: Higher natural frequency vs the axial compressive forces (F_1 and F_2).

Table 3: The natural frequencies vs the axial compressive forces (F_1 and F_2)

Axial compressive force (N)	PP Beam		CC Beam		CF Beam		CP Beam	
	L	*H*	*L*	*H*	*L*	*H*	*L*	*H*
2,000	27.4866	103.7088	62.93775	118.1574	9.4655	100.4470	43.2188	108.9397
3,000	27.2361	103.6427	62.69041	118.0258	9.2039	100.4227	42.9703	108.8414
4,000	26.9833	103.5765	62.44208	117.8941	8.9347	100.3984	42.7204	108.7430
5,000	26.7281	103.5103	62.19276	117.7622	8.6571	100.3740	42.4690	108.6445
6,000	26.4704	103.4441	61.94243	117.6302	8.3703	100.3497	42.2162	108.5459
7,000	26.2102	103.3778	61.69109	117.498	8.0733	100.3254	41.9618	108.4472
8,000	25.9474	103.3115	61.43872	117.3657	7.7650	100.3010	41.7058	108.3484
9,000	25.6819	103.2451	61.18532	117.2333	7.4439	100.2767	41.4483	108.2496
10,000	25.4136	103.1787	60.93085	117.1007	7.1084	100.2523	41.1892	108.1506
11,000	25.1425	103.1123	60.67532	116.9679	6.7561	100.2280	40.9284	108.0515
12,000	24.8684	103.0458	60.41871	116.835	6.3845	100.2036	40.6659	107.9524
13,000	24.5912	102.9793	60.16101	116.702	5.9899	100.1792	40.4018	107.8532
14,000	24.3109	102.9127	59.90219	116.5687	5.5674	100.1549	40.1359	107.7539
15,000	24.0273	102.8461	59.64226	116.4354	5.1100	100.1305	39.8682	107.6544
16,000	23.7403	102.7794	59.38118	116.3019	4.6075	100.1061	39.5988	107.5549
17,000	23.4499	102.7127	59.11895	116.1682	4.0430	100.0817	39.3275	107.4553
18,000	23.1557	102.6459	58.85556	116.0344	3.3856	100.0573	39.0542	107.3557
19,000	22.8578	102.5792	58.59098	115.9004	2.5650	100.0329	38.7791	107.2559
20,000	22.5560	102.5123	58.3252	115.7663	1.3023	100.0085	38.5020	107.1560

$\rho_1 = \rho_2 = 2{,}000\ \mathrm{kg/m^3}$, $E_1 = E_2 = 1 \times 10^{11}\ \mathrm{N/m^2}$, $K = 10^5\ \mathrm{N/m^2}$, $L = 6$ m, $b = 0.2$ m, and $h = 0.05$ m.

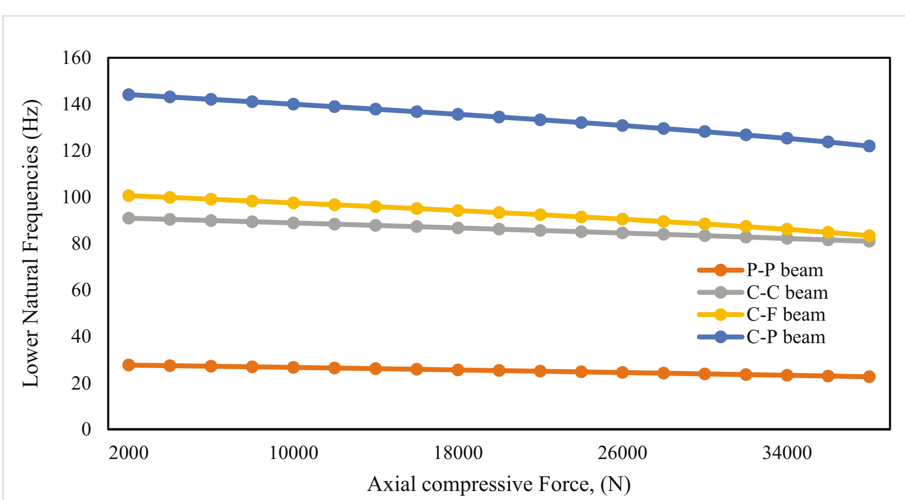

Figure 6: Lower natural frequency vs the axial compressive forces ($F_2 = 0$).

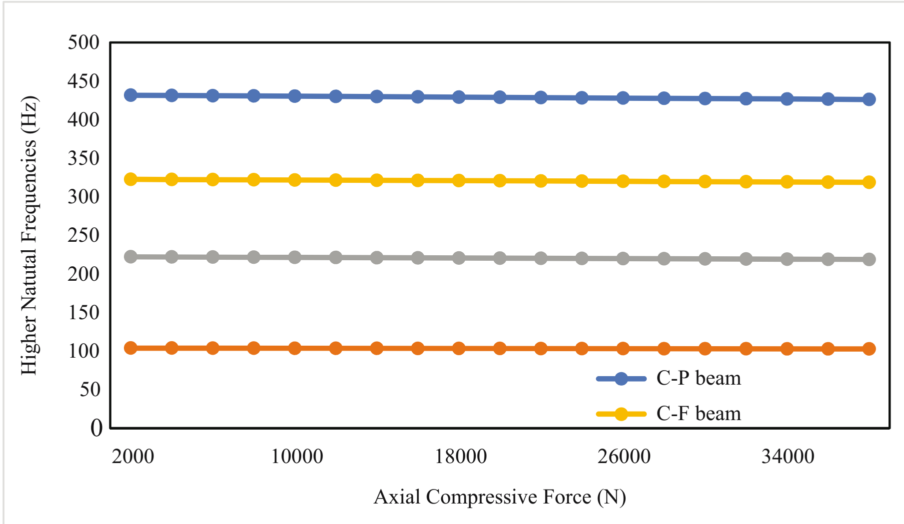

Figure 7: Lower natural frequency vs the axial compressive forces.

clamped. This may be due to the buckling effect of the compressive axial force, so the more serious effect of the axial force is expected on natural frequencies when both ends are free. It was also noticed that the change in compressive force affects the lower natural frequencies (synchronous), while its effect is almost non-existent on the higher natural frequencies (asynchronous).

4 Conclusions

When the axial compressive force is increased from 2,000 to 38,000 N, it is noted that the lower natural frequencies decreased by 19% for the PP beam, 8% for the CC beam, 81% for the CF beam, and by 12% for the CP beam. While it is noticed that the greatest effect of the axial force on

Table 4: The natural frequencies vs the axial compressive force ($F_2 = 0$)

F_1 (N)	PP Beam		CC Beam		CF Beam		CP Beam	
	L	*H*	*L*	*H*	*L*	*H*	*L*	*H*
2,000	27.73453	103.775	63.18337	118.2892	9.719947	100.4713	43.4653	109.0382
4,000	27.48527	103.7092	62.93469	118.159	9.465034	100.447	43.21668	108.9406
6,000	27.23304	103.6435	62.68347	118.0295	9.202803	100.4228	42.96554	108.8433
8,000	26.97775	103.578	62.42971	117.9006	8.932611	100.3985	42.71185	108.7464
1,0000	26.71932	103.5126	62.17335	117.7725	8.653712	100.3743	42.45557	108.6498
1,2000	26.45766	103.4474	61.91438	117.645	8.365234	100.3501	42.19665	108.5535
14,000	26.19267	103.3823	61.65275	117.5182	8.066151	100.326	41.93504	108.4575
16,000	25.92424	103.3173	61.38844	117.392	7.755235	100.3018	41.67068	108.362
18,000	25.65227	103.2525	61.12142	117.2666	7.431001	100.2776	41.40353	108.2667
20,000	25.37665	103.1878	60.85164	117.1419	7.091622	100.2535	41.13353	108.1718
22,000	25.09725	103.1233	60.57908	117.0178	6.734811	100.2294	40.86063	108.0772
24,000	24.81396	103.0589	60.30369	116.8944	6.357632	100.2053	40.58477	107.983
26,000	24.52662	102.9947	60.02545	116.7717	5.956216	100.1812	40.30589	107.8891
28,000	24.23511	102.9306	59.74431	116.6497	5.525285	100.1572	40.02393	107.7955
30,000	23.93926	102.8666	59.46024	116.5284	5.057299	100.1332	39.73881	107.7023
32,000	23.63892	102.8028	59.17319	116.4078	4.540815	100.1091	39.45048	107.6094
34,000	23.3339	102.7391	58.88313	116.2879	3.956888	100.0851	39.15887	107.5169
36,000	23.02404	102.6756	58.59001	116.1687	3.26958	100.0612	38.86389	107.4247
38,000	22.70912	102.6122	58.29379	116.0502	2.391355	100.0372	38.56549	107.3329

$\rho_1 = \rho_2 = 2{,}000$ kg/m^3, $E_1 = E_2 = 1 \times 10^{11}$ N/m^2, $K = 10^5$ N/m^2, $L = 6$ m, $b = 0.2$ m, and $h = 0.05$ m.

the higher natural frequencies is by reducing it in the CC beam by a ratio that does not exceed 2%. A rise in the axial force causes a lessening in the lower natural frequencies, especially for the CF beam, while it has a small influence on the higher natural frequencies. Similarly, when the compressive forces on the upper and lower beams fluctuate at the same time, their effect is doubled on the frequencies when the axial compressive force on one of the two beams changes only. The natural frequencies change in the same proportion when the axial compressive force on one of the two beams changes, whether it is the upper or lower, and the value of the axial force remains constant on the other beam.

In this study, when both the upper and lower layers of the double beam are fixed symmetrically, it was found that the axial force has a significant effect on the lower natural frequencies (synchronous) and its effect is minimal on the higher natural frequencies (asynchronous), especially when one or both ends of the beam are free. In the future, it is important to study the change in the boundary conditions for the connection of the upper and lower layers to be asymmetrical by stabilization and the effect of this on the natural frequencies.

Conflict of interest: Authors state no conflict of interest.

References

[1] Zhang YQ, Lu Y, Ma GW. Effect of compressive axial load on forced transverse vibrations of a double-beam system. Int J Mech Sci. 2008;50(2):299–305. doi: 10.1016/j.ijmecsci.2007.06.003.

[2] Zhang YQ, Lu Y, Wang SL, Liu X. Vibration and buckling of a double-beam system under compressive axial loading. J Sound Vib. 2008;318(1–2):341–52. doi: 10.1016/j.jsv.2008.03.055.

[3] Zhao X, Chen B, Li YH, Zhu WD, Nkiegaing FJ, Shao YB. Forced vibration analysis of Timoshenko double-beam system under compressive axial load by means of Green's functions. J Sound Vib. 2019;464:115001. doi: 10.1016/j.jsv.2019.115001.

[4] Zhao X. Solution to vibrations of double-beam systems under general boundary conditions. J Eng Mech. 2021;147(10):04021073. doi: 10.1061/(ASCE)EM.1943-7889.0001953.

[5] Zhao X, Chang P. Free and forced vibration of double beam with arbitrary end conditions connected with a viscoelastic layer and discrete points. Int J Mech Sci. 2021;209:106707. doi: 10.1016/j.ijmecsci.2021.106707.

[6] Mao Q, Wattanasakulpong N. Vibration and stability of a double-beam system interconnected by an elastic foundation under conservative and nonconservative axial forces. Int J Mech Sci. 2015;93:1–7. doi: 10.1016/j.ijmecsci.2014.12.019.

[7] Mao Q. Free vibration analysis of elastically connected multiple-beams by using the Adomian modified decomposition method. J Sound Vib. 2012;331(11):2532–42. doi: 10.1016/j.jsv.2012.01.028.

[8] Fei H, Danhui D, Cheng W, Jia P. Analysis on the dynamic characteristic of a tensioned double-beam system with a semi theoretical semi numerical method. Compos Struct. 2017;185:S0263822317304968. doi: 10.1016/j.compstruct.2017.11.010.

[9] Fei H, Danhui D, Wei C, Jubao Z. A novel analysis method for damping characteristic of a type of double-beam systems with viscoelastic layer. Appl Math Model. 2020;80:911–28. doi: 10.1016/j.apm.2019.11.008.

[10] Fei H, Danhui D, Zichen D. A dynamic stiffness-based modal analysis method for a double-beam system with elastic supports. Mech Syst Signal Process. 2021;146:106978. doi: 10.1016/j.ymssp.2020.106978.

[11] Sari ME, Al-Kouz WG, Al-Waked R. Bending–torsional-coupled vibrations and buckling characteristics of single and double composite Timoshenko beams. Adv Mech Eng. 2019;11(3):168781401983445. doi: 10.1177/1687814019834452.

[12] Stojanović V, Kozić P, Pavlović R, Janevski G. Effect of rotary inertia and shear on vibration and buckling of a double beam system under compressive axial loading. 2011;81(12):1993–2005. doi: 10.1007/s00419-011-0532-1.

[13] Stojanović V, Kozić P. Forced transverse vibration of Rayleigh and Timoshenko double-beam system with effect of compressive axial load. Int J Mech Sci. 2012;60(1):59–71. doi: 10.1016/j.ijmecsci.2012.04.009.

[14] Kozić P, Pavlović R, Karličić D. The flexural vibration and buckling of the elastically connected parallel-beams with a Kerr-type layer in between. Mech Res Commun. 2014;56:83–9. doi: 10.1016/j.mechrescom.2013.12.003.

[15] Abdulsahib IA, abbas Atiyah Q. Effects of internal connecting layer properties on the vibrations of double beams at different boundary conditions. J Mech Eng Res Dev. 2020;43:289–96.

[16] Abdulsahib IA, abbas Atiyah Q. Vibration analysis of a symmetric double-beam with an elastic middle layer at arbitrary boundary conditions. Math Model Eng Probl. 2022;9(4):1136–42. doi: 10.18280/mmep.090433.

[17] Milenković B, Karličić D, Jovanović Đ. Determination of natural frequency and amplitude ratio of a Rayleigh double beam system with a Keer middle layer subjected to compressive axial load; XI International Conference Industrial Engineering and Environmental Protection; 2021. (IIZS 2021).

[18] Abbas Atiyah Q, Abdulsahib IA. Effects of geometrical and material properties on vibrations of double beams at different boundary conditions. J Mech Eng Res Dev. 2020;43(7):310–25.

[19] Abbas Atiyah Q, Abdulsahib IA. The behavior of the synchronous and asynchronous natural frequencies for asymmetric double beams. Math Model Eng Probl. 2022;9(5):1243–50. doi: 10.18280/mmep.090511